

Non-algebraic entanglement growth in long-range many-body localized systems

Rozhin Yousefjani,^{1,*} Sougato Bose,^{2,†} and Abolfazl Bayat^{1,‡}

¹*Institute of Fundamental and Frontier Sciences, University of Electronic Science and Technology of China, Chengdu 610051, China*

²*Department of Physics and Astronomy, University College London, Gower Street, London WC1E 6BT, United Kingdom*

The fate of many-body localization in long-range interacting systems is not fully settled and several open problems still exist. For instance, the phase boundary between ergodic and many-body localized regimes has yet to be fully determined. In addition, the dynamical growth of entanglement in the many-body localized phase of such systems is under debate. Here, we introduce a Floquet dynamics which can induce many-body localization in a disorder-free long-range interacting system through temporal random local rotations. The phase diagram has been determined for two types of long-range couplings. Interestingly, our Floquet mechanism shows more localizing power than conventional static disorder methods as it pushes the phase transition boundary in favor of the many-body localized phase. Moreover, our comprehensive long-time simulations reveal that in long-range many-body localized systems the entanglement grows as $\sim (\ln t)^\gamma$ (for some constant γ). This is in sharp contrast with the conjecture of algebraic growth, in previous perturbative studies, and can smoothly recover the well-known logarithmic entanglement growth in short-range interacting systems.

Introduction.— Many-Body Localization (MBL) is a profound concept in condensed matter physics for breaking the ergodicity principle[1–9]. To better understand the different aspects of MBL, several quantum information concepts [10–16] have been theoretically developed and several experiments on newly emerging quantum simulators have been performed [17–33]. Most of the MBL literature have been dedicated to 1D short-range interactions, however, several fundamental problems remain open for systems with long-range couplings [34, 35]. These systems are very relevant as many interactions in nature are inherently long-ranged and certain quantum simulators, e.g. ion-traps [17, 18, 36] and Rydberg atoms [19–21], are naturally governed by long-range interactions between their particles. Long-range couplings can exist in various forms, e.g. tunneling or Ising-type interactions, which may affect the MBL physics very differently. In fact, one challenging issue in such systems is to extract the precise ergodic-MBL phase diagram [37–48].

Another open problem is the exact form of the growth of entanglement entropy during the dynamics of a long-range MBL system. In short-range (i.e. nearest-neighbor) Anderson localized systems the entanglement entropy, after a short period of rising, saturates to a constant value [49]. In the absence of interaction, by continuously changing the power-law tunneling from short- to long-range the entanglement entropy grows algebraically $\sim t^\gamma$ [37, 50, 51], with γ increasing from 0 (short-range) to finite values (long-range). The situation becomes far more complex in the presence of power-law interaction. While the short-range MBL systems show logarithmic growth of entanglement entropy [52], the situation in long-range cases have not yet been resolved. By introducing perturbatively small Ising interactions to a system with long-range tunnelings, the growth of entanglement entropy in the MBL phase remains algebraic [53, 54]. In Ref. [37], it has been shown that at the MBL-ergodic transition point the entanglement entropy grows algebraically with a universal exponent, even for non-perturbative long-range models. Based on these, it has been conjectured, through short-time simulations, that algebraic growth of entanglement may remain valid in the

MBL phase as well for arbitrary strengths of interaction [55–57]. However, unlike the case for long-range tunneling without interaction, this conjecture fails to smoothly recover the logarithmic growth of entanglement for short-range MBL systems. Since the dynamics is always taking place in the MBL phase, without going through any phase transition, the smooth continuity between the short- and long-range interactions is indeed expected.

Periodically driving many-body interacting systems, known as Floquet dynamics, is a well-known mechanism for thermalizing the system [58, 59], a phenomenon opposite to MBL. The fate of MBL systems under different Floquet dynamics have been studied in both theory [60–67] and experiments [31]. The results show that the MBL does not survive the Floquet dynamics unless the energy cannot be absorbed by the system due to either high frequency or large amplitude of the driving field [31, 61]. In a remarkably different approach, in Refs. [68–70] the Floquet dynamics is designed to suppress the tunneling of the particles in a weakly disordered system to enhance the relative strength of disorder and interaction for generating an MBL phase. One may wonder whether it is possible to induce MBL through temporal random rotations without introducing static disorder in the Hamiltonian of the system. Apart from being fundamentally interesting, this has practical advantages too. In fact, inducing static disorder may result in leakage from the valid Hilbert space in superconducting quantum simulators or heating in ion-trap systems. These issues make experiments very challenging in the deep MBL phase [22].

In this letter, inspired by Quantum Approximate Optimization Algorithm (QAOA), we introduce a Floquet mechanism that can generate an MBL phase for a disorder-free Hamiltonian. We fully determine the phase diagram of the system and show that our mechanism can induce MBL in certain long-range systems which cannot be localized by disordered Hamiltonians. This observation gets more support through monitoring the dynamical evolution of imbalance. Remarkably, through extensive long-time numerical simulations, we show that in long-range MBL systems the entanglement en-

tropy does not grow algebraically, as conjectured previously, and follows $(\log t)^\gamma$ behavior. This can smoothly recover the logarithmic growth in the short-range interaction limit.

Model.— We consider a spin-1/2 chain of L particles interacting with long-range tunneling and Ising interaction

$$H = - \sum_{i \neq j} \left\{ \frac{J_x}{|i-j|^a} (S_i^x S_j^x + S_i^y S_j^y) + \frac{J_z}{|i-j|^b} S_i^z S_j^z \right\}. \quad (1)$$

Here $S_i^{(x,y,z)}$ is the spin-1/2 operator for qubit at site i , $J_x=J_z=1$ are the interaction strengths, and $a, b > 0$ are the power-law exponents which determine the range of the tunneling and interaction, respectively. By varying these exponents one can tune the interaction geometry from a fully connected graph (for exponents being 0) to a local nearest-neighbor 1D chain (when the exponents tend to ∞). These long-range couplings can now be realized in ion trap [71, 72] systems. Many types of long-range models [34, 35] such as Coulomb, van der Waals and dipole-dipole interactions, are special cases of Hamiltonian H . We systematically investigate two different regimes: (i) uniform couplings in which $a=b$; and (ii) nonuniform couplings in which b is finite (power-law Ising interaction) and $a \rightarrow \infty$ (nearest-neighbor tunneling).

Note that the Hamiltonian H is disorder-free and thus naturally ergodic. Even performing Floquet dynamical decoupling methods [68–70] cannot induce MBL in this system. In order to dynamically localize this Hamiltonian, we need a different approach. We propose a Floquet dynamics in which the evolution over a single time period τ consists of two operations. First, the system evolves under the action of the clean Hamiltonian H for a short-time period τ . Second, an instant kick operation which is a set of local rotations along the \hat{z} axis, i.e. $\mathcal{R}(\theta) = \prod_{i=1}^L e^{-i\theta_i S_i^z}$, rotates all the qubits without creating excitations in the system. The random angles $\theta = (\theta_1, \dots, \theta_L)$ are drawn from a uniform distribution $[-\theta/2, \theta/2]$ with $0 \leq \theta/\pi \leq 1$ being the strength of the kick. Hence, the evolution operator over a single period becomes

$$U_F(\theta, \tau, a, b) = \mathcal{R}(\theta) e^{-iH\tau}. \quad (2)$$

Note that the random angles θ remain fixed in different periods. The random kick operator $\mathcal{R}(\theta)$ affects the dynamics of the system to be described by an effective Hamiltonian H_F such that $U_F = e^{-iH_F\tau}$. The random nature of θ prevent us from analytically driving a closed form for H_F restricting us to numerical simulations.

Phase diagram (uniform case).— Since the dynamics of the system is described by the effective Hamiltonian H_F , one can investigate the properties of this Hamiltonian to determine the phase diagram of the system as a function of parameters (θ, τ, a, b) . We first investigate the statistical properties of energy levels of H_F , namely $\{E_k\}$, or equivalently the quasi-energy levels of U_F given by $\{e^{-iE_k\tau}\}$. Numerically, we compute the quasi-energies using exact diagonalization of U_F in the subspace of vanishing total $S_z = \sum_j S_j^z$ and all the results are averaged over 1000 random samples of θ to guarantee proper convergence. Since the Hamiltonian in Eq.(1),

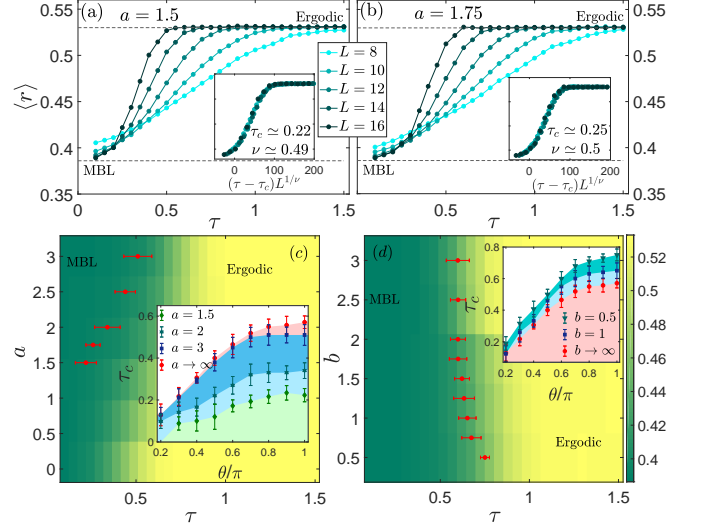


FIG. 1: **Upper panels:** Random-averaged level statistics ratio $\langle r \rangle$ as a function of τ for uniform couplings: (a) $a=b=1.5$; and (b) $a=b=1.75$. In both panels, the results are obtained for fixed $\theta=\pi$ in systems with various sizes and the dashed lines corresponds to $\langle r \rangle \approx 0.529$ and $\langle r \rangle \approx 0.386$ for ergodic and MBL phases, respectively. The insets are the finite-size scaling analysis for extracting τ_c and ν . **Lower panels:** Phase diagram of the system, obtained via finite-size scaling of $\langle r \rangle$ in a system with $L = 16$ and $\theta = \pi$, as a function of τ for: (c) uniform couplings ($a = b$); and (d) nonuniform couplings ($b \ll a \rightarrow \infty$). In both panels, the red markers show the MBL-ergodic phase boundary. The inset of panel (c) shows the critical τ_c as a function of θ for various choices of a in a uniform chain. The inset of panel (d) depicts τ_c as a function of θ for various choices of b in a nonuniform chain. In both insets, the area below each curve represents the MBL phase.

and thus its corresponding H_F , is dramatically less sparse than the nearest-neighbor interactions our numerical simulations are restricted up to $L=16$. By computing the consecutive energy gaps $\delta_k = E_{k+1} - E_k$, one can characterize the level statistics by their ratio $r_k = \min(\delta_{k+1}, \delta_k) / \max(\delta_{k+1}, \delta_k)$. The averaged value of this ratio, $\langle r \rangle$, serves as a well-established tool in numerical studies of finite MBL systems [73]. While the MBL phase is determined by Poisson level statistics with $\langle r \rangle \approx 0.386$, the ergodic phase is known to follow the circular orthogonal ensemble level statistics with $\langle r \rangle \approx 0.529$ [6, 74].

Clearly, we have four control parameters in the system, namely (θ, τ, a, b) , which determine whether the system is ergodic or MBL. For every choice of these parameters, one can compute $\langle r \rangle$ to reveal the phase of the system. As an example, by fixing $\theta = \pi$ and considering various system sizes, in Figs. 1(a)-(b), we plot $\langle r \rangle$ as a function of τ for two choices of uniform couplings $a = b = 1.5$ and $a = b = 1.75$, respectively. Two major features can be observed. First, as τ increases the system becomes ergodic and this transition gets sharper by increasing the system size. This can be understood as the disorder-free Hamiltonian H is ergodic and by increasing τ its evolution gets enough time to thermalize the system. In other words, the effective Hamiltonian H_F is dominantly

determined by the Hamiltonian H rather than the disordered kick operator $\mathcal{R}(\theta)$. Second, the curves for different sizes intersect at a specific τ , which indicates the transition point τ_c . However, due to the finite-size effect, small fluctuations are always observed for the intersection of different curves, making it imprecise for extracting the transition point. Therefore, to precisely determine the phase boundary, we perform a finite-size scaling analysis and find the transition point τ_c and the critical exponent ν such that all the curves of $\langle r \rangle$ collapse on a universal one as they are plotted as a function of $(\tau - \tau_c)L^{1/\nu}$. The results, computed by the Python package `pyfssa` [75, 76], are shown in the inset of Figs. 1(a)-(b) which give $\tau_c = 0.22$ and $\tau_c = 0.25$ for $a = 1.5$ and $a = 1.75$, respectively.

The analysis of Figs. 1(a)-(b), can be repeated for other choices of the control parameters. Remarkably, for $a < 1.5$ the curves for $\langle r \rangle$ do not show a clear intersection and the finite-size scaling analysis fails to collapse the curves, for all choices of other parameters, indicating the absence of MBL transition, see the Supplementary Materials (SM) for more details. This shows that for long-range tunneling couplings below $a_c \simeq 1.5$ the MBL never happens, in the considered system sizes. This is a very interesting observation as the power-law couplings a and b play two opposite roles. Decreasing the coupling a allows spin tunneling between the distant qubits which enhances ergodicity. On the other hand, decreasing the coupling b creates an effective random magnetic field at each site as every spin configuration of the system contributes a different energy shift to that site, thanks to the long-range Ising interaction. The absence of MBL in uniform couplings (i.e. $a = b$) for $a < a_c \simeq 1.5$ shows that the thermalizing long-range tunneling overcomes the localizing long-range Ising. This has also been observed in ordinary disordered long-range Hamiltonians. However, while in such systems a_c is found to be $a_c \simeq 2$ [37, 40, 55], our Floquet system shows more localization power with $a_c \simeq 1.5$. In other words, the temporal disorder $\mathcal{R}(\theta)$ has more localization power than the spatial one. This issue will be further discussed in the following sections.

To investigate the phase diagram of the uniform case (i.e. $a=b$) with more details, we keep the strength of the random kick to a strong value of $\theta = \pi$ and plot $\langle r \rangle$ as a function of a and τ in Fig. 1(c) for system of size $L = 16$. The boundary between the ergodic and the MBL phases, denoted by red markers, is determined by finite-size scaling analysis of $\langle r \rangle$, as discussed before. The figure clearly shows that for a smaller than $a_c \simeq 1.5$ the considered systems (up to size $L = 16$) never localizes even for small τ 's and a strong disorder kick with $\theta = \pi$. In addition, to clarify the role of random kick strength, in the inset of Fig. 1(c) we plot the critical time τ_c as a function of θ for various a . The area below each curve represents the MBL phase. Clearly, by reducing a the MBL area shrinks showing the tendency towards thermalization.

Phase diagram (nonuniform case).— To determine the phase diagram of the system for nonuniform couplings ($b \ll a \rightarrow \infty$), in Fig. 1(d), we plot $\langle r \rangle$ as a function of b and τ in a system of size $L = 16$, when the strength of the disordered kick is fixed to $\theta = \pi$. The phase boundary between the MBL

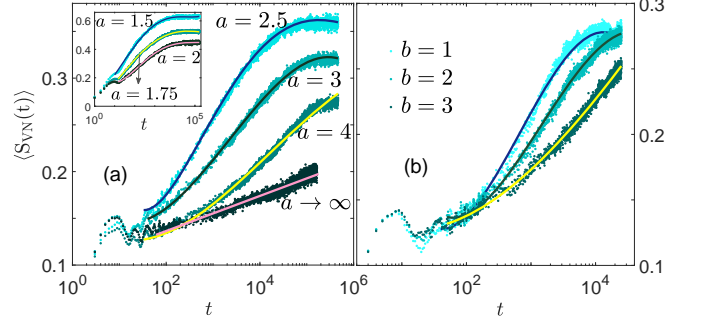


FIG. 2: (a) and its inset: $\langle S_{VN}(t) \rangle$ as a function of t in the MBL phase for uniform couplings (i.e. $a=b$). (b) $\langle S_{VN}(n) \rangle$ as a function of t in the MBL phase for nonuniform couplings (i.e. $b \ll a \rightarrow \infty$) couplings. In both panels, $\theta=\pi$, $\tau=0.1$ and $L=16$ and the solid lines correspond to the best fitting function of the form $\langle S_{VN}(t) \rangle \propto (\ln t)^\gamma$ with γ 's given in Table I.

and the ergodic phases are denoted by red markers. Interestingly, by decreasing b (i.e. making the Ising interaction more long-range) the localization power increases and the system can localize for longer τ . This can be understood as for every spin configuration the Ising interaction induces a different effective energy shift to each qubit, similar to a local magnetic field. Therefore, by having a superposition of different spin configurations every qubit feels an effective random field which assists localization just as a spatially disordered magnetic field. To see the effect of disordered kick strength on the phase diagram, in the inset of Fig. 1(d) we plot τ_c as a function of θ for various b . The area below the curves represents the MBL phase. As expected, by decreasing b the MBL region increases confirming that the localization power is enhanced.

Dynamical analysis of the MBL phase.— Despite being very useful for determining the phase diagram, the level statistics analysis cannot fully reveal the profound underlying MBL physics in our long-range many-body system. In fact, it is highly insightful to investigate the dynamical properties of the system within the MBL phase by focusing on two quantities, namely entanglement entropy and imbalance. Two major objectives are pursued : (i) addressing the inconsistency of the MBL dynamics of entanglement entropy when the interaction continuously changes from short-range to long-range; and (ii) providing further affirmation for true existence of the MBL regime in the phase diagram extracted from the level statistic.

A system of size $L = 16$ is initialized in Néel state $|\psi(0)\rangle = |\uparrow\downarrow \dots \uparrow\downarrow\rangle$. For fixed $\theta=\pi$ and $\tau=0.1$, the evolution of the system after t times kicking is given by $|\psi(t)\rangle = (U_F)^t |\psi(0)\rangle$. Entanglement entropy is defined as $S_{VN}(t) = -\text{Tr}[\rho_{L/2}(t) \ln \rho_{L/2}(t)]$, where $\rho_{L/2}(t)$ is the reduced density matrix of the state $|\psi(t)\rangle$ when the right half is traced out. On the other hand, imbalance is defined as $I(t) = 2/L \sum_i (-1)^{i+1} \langle S_i^z \rangle$, where $\langle S_i^z \rangle = \langle \psi(t) | S_i^z | \psi(t) \rangle$ and the normalization in the definition guarantees that $I(0)=1$. In the following, after averaging these quantities over 1000 random samples we denote these quantities as $\langle S_{VN}(t) \rangle$ and $\langle I(t) \rangle$.

Entanglement entropy growth.— In the ergodic phase, both

a	1.5	1.75	2.00	2.50	3.0	4.0	∞	b	1.0	2.0	3.0
$\gamma \approx$	4.0	3.54	3.52	3.51	3.0	2.5	1.0	$\gamma \approx$	3.0	2.5	2.0

TABLE I: The exponent γ of the fitting function $\langle S_{VN} \rangle \sim (\ln t)^\gamma$ as a function of a (b) in the left (right) table for the uniform (nonuniform) couplings.

interacting ($J_z > 0$) and non-interacting ($J_z = 0$) systems show linear growth of entanglement entropy, namely $S_{VN} \sim t$, until it saturates to a volume-law value [77]. In localized disordered systems with long-range tunneling and $J_z = 0$ the entanglement entropy grows algebraically, namely t^γ (for some constant γ) [37, 50, 51] as in such systems the Local Integrals of Motions (LIOMs) localize algebraically [54]. By continuously increasing a one can recover Anderson localization in the short-range limit ($a \rightarrow \infty$) for which $\gamma=0$ and the entanglement entropy does not grow in time [77].

The situation is remarkably different when $J_z > 0$. In short-range MBL systems the entanglement entropy grows logarithmically in time, namely $S_{VN} \sim \ln t$. For long-range systems, the growth of entanglement entropy is still not understood. In Ref. [54] the algebraically localized LIOMs in the case of $J_z = 0$ are perturbatively studied for the case of $0 < J_z \ll 1$ and it was concluded that the same algebraic localization behavior may be observed in this limit. Thus, similar to the case of $J_z = 0$, the entanglement entropy may grow algebraically t^γ , which was confirmed in some numerical studies too [53, 54]. For non-perturbative regime (i.e. $J_z \approx 1$), in Ref. [55], the authors perform a short-time matrix product state evolution for a long-range MBL system and conjectured that the entanglement entropy growth might be algebraic. However, if this conjecture is valid, one fails to recover the logarithmic growth of entanglement entropy from the algebraic behavior as a continuously increases to short-range interaction (i.e. $a \rightarrow \infty$). This is in sharp contrast with the case of $J_z = 0$, discussed above, where one can continuously transform the behavior of entanglement entropy between the short- and long-range interactions. Note that the continuity is expected as the system remains in the MBL phase and does not go through any phase transition.

Astonishingly, our numerical simulations in the non-perturbative regime (i.e. $J_z = 1$) do not match with an algebraic growth of entanglement entropy and indeed well fit with $S_{VN} \sim (\ln t)^\gamma$, which can also continuously recover the short-range behavior with $\gamma = 1$ as $a \rightarrow \infty$. We highlight this observation as the key result of this letter. To show this, in Fig. 2(a) and its inset, we plot $\langle S_{VN}(t) \rangle$ as a function of t for a uniform coupling (i.e. $a = b$) and various choices of a . One can easily see that $S_{VN} \sim (\ln t)^\gamma + O((\ln t)^{\gamma-1})$ fits very well with numerical data over a very long simulation time ($t \sim 10^6$). By decreasing a one can see that the entanglement growth becomes faster (γ gets larger) and the entropy saturates to a higher value. For the sake of clarity, some of the curves are shown in the inset of Fig. 2(a). For the case of nonuniform couplings (i.e. $b \ll a \rightarrow \infty$) we plot $\langle S_{VN}(t) \rangle$ as a function of t for various choices of b in Fig. 2(b). Re-

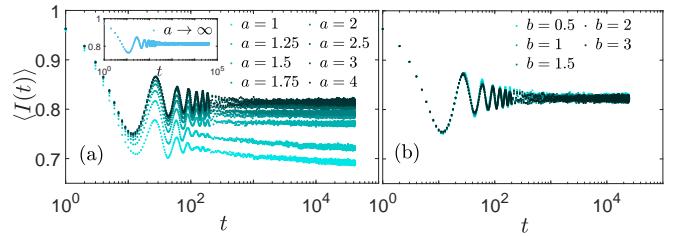


FIG. 3: Imbalance $\langle I(t) \rangle$ versus t in the MBL phase for $\theta=\pi$, $\tau=0.1$ and $L=16$. Panel (a) and its inset are for the uniform couplings ($a=b$). Panel (b) is for the nonuniform couplings ($b \ll a \rightarrow \infty$).

markably, the same fitting function $S_{VN} \sim (\ln t)^\gamma$ provides the most precise description of the data. The intuitive observation is that decreasing b makes the speed of the entanglement entropy growth faster (namely larger γ), however, the saturation value looks slightly smaller showing more localization. For the sake of completeness, in Table I, we provide the estimated values of γ for both uniform and nonuniform couplings [38].

Dynamics of Imbalance.— While in the ergodic phase, the imbalance has to saturate to zero, showing no memory about the initial state, in the MBL phase it reaches a finite value, resembling the memory of its initial state [13, 28, 31]. Fig. 3 illustrates random-averaged imbalance versus t for: (a) uniform; and (b) nonuniform couplings. After a transition time, the imbalance relaxes to a plateau for $a \geq 1.5$ in Fig. 3(a) signaling the MBL phase, which is in full agreement with the level statistics analysis. Remarkably, for $a < 1.5$ the imbalance never reaches a plateau and continuously goes down, signaling ergodicity. This confirms that for the choice of $\tau = 0.1$, $\theta = \pi$ the critical power-law coupling is $a_c \simeq 1.5$, again in agreement with level statistics analysis. For nonuniform couplings (i.e. $b \ll a \rightarrow \infty$), in Fig. 3(b), we plot the imbalance as a function of t for various b 's. All the curves, clearly show the MBL phase and the saturation values are very close to each other, showing that in localized system the saturation of imbalance hardly changes by b .

Conclusion.— We have proposed a Floquet mechanism, inspired by actively used QAOA experiments in quantum simulators, which enables the creation of the MBL phase in a disorder-free long-range interacting system. In the limit of short-time evolution τ , the mechanism reproduces the results for disordered systems. By utilizing this Floquet mechanism, two main results have been achieved. Firstly, we have determined the phase diagram of the system for two different types of couplings, uniform ($a = b$) and nonuniform ($b \ll a \rightarrow \infty$). Our mechanism shows a strong localizing power such that it can prevent thermalization in those long-range systems which cannot be localized merely by disorder. Secondly, we have revealed that the entanglement entropy grows as $\sim (\ln t)^\gamma$ in the MBL phase of long-range interacting systems. This not only challenges the previous conjecture of algebraic growth of entanglement, mainly based on perturbative analysis, but also allows the smooth recovery of logarithmic growth of entanglement in the short-range MBL systems.

Acknowledgments.— AB acknowledges support from the National Key R&D Program of China (Grant No. 2018YFA0306703), National Science Foundation of China (Grants No. 12050410253 and No. 92065115) and the Ministry of Science and Technology of China for the Young Scholars National Foreign Expert Project (Grant No. QNJ2021167001L). SB acknowledges the EPSRC grant for nonergodic quantum manipulation (Grant No. EP/R029075/1).

^{*} Electronic address: RozhinYousefjani@uestc.edu.cn
[†] Electronic address: s.bose@ucl.ac.uk
[‡] Electronic address: abolfazl.bayat@uestc.edu.cn

[1] E. Altman, *Nat. Phys.* **14**, 979 (2018).
[2] D. A. Abanin and Z. Papić, *Annalen der Phys.* **529**, 1700169 (2017).
[3] M. Serbyn, Z. Papić, and D. A. Abanin, *Phys. Rev. Lett.* **111**, 127201 (2013).
[4] M. Serbyn, Z. Papić, and D. A. Abanin, *Phys. Rev. Lett.* **111**, 127201 (2013).
[5] D. A. Abanin, E. Altman, I. Bloch, and M. Serbyn, *Rev. Mod. Phys.* **91** (2019).
[6] D. J. Luitz, N. Laflorencie, and F. Alet, *Phys. Rev. B* **91**, 1 (2015).
[7] V. Khemani, S. P. Lim, D. N. Sheng, and D. A. Huse, *Phys. Rev. X* **7**, 1 (2017).
[8] A. Pal and D. A. Huse, *Phys. Rev. B* **82**, 174411 (2010).
[9] S. Iyer, V. Oganesyan, G. Refael, and D. A. Huse, *Phys. Rev. B* **87**, 134202 (2013).
[10] J. Gray, S. Bose, and A. Bayat, *Phys. Rev. B* **97**, 201105 (2018).
[11] J. Gray, A. Bayat, A. Pal, and S. Bose, arXiv:1908.02761.
[12] A. Nico-Katz, A. Bayat, and S. Bose, arXiv:2009.04470.
[13] A. Nico-Katz, A. Bayat, and S. Bose, arXiv:2111.01146.
[14] G. De Tomasi, S. Bera, J. H. Bardarson, and F. Pollmann, *Phys. Rev. Lett.* **118**, 016804 (2017).
[15] Z.-H. Sun, J. Cui, and H. Fan, *Phys. Rev. Research* **2**, 013163 (2020).
[16] M. Kiefer-Emmanouilidis, R. Unanyan, M. Fleischhauer, and J. Sirker, *Phys. Rev. Lett.* **124**, 243601 (2020).
[17] J. Smith, A. Lee, P. Richerme, B. Neyenhuis, P. W. Hess, P. Hauke, M. Heyl, D. A. Huse, and C. Monroe, *Nat. Phys.* **12**, 907 (2016).
[18] W. Morong, F. Liu, P. Becker, K. S. Collins, L. Feng, A. Kyprianidis, G. Pagano, T. You, A. V. Gorshkov, and C. Monroe, *Nature* **599**, 393 (2021).
[19] J.-y. Choi, S. Hild, J. Zeiher, P. Schauß, A. Rubio-Abadal, T. Yefsah, V. Khemani, D. A. Huse, I. Bloch, and C. Gross, *Science* **352**, 1547 (2016).
[20] M. Rispoli, A. Lukin, R. Schittko, S. Kim, M. E. Tai, J. Léonard, and M. Greiner, *Nature* **573**, 385 (2019).
[21] A. Lukin, M. Rispoli, R. Schittko, M. E. Tai, A. M. Kaufman, S. Choi, V. Khemani, J. Léonard, and M. Greiner, *Science* **364**, 256 (2019).
[22] M. Gong, G. D. de Moraes Neto, C. Zha, Y. Wu, H. Rong, Y. Ye, S. Li, Q. Zhu, S. Wang, Y. Zhao, et al., *Phys. Rev. Research* **3**, 033043 (2021).
[23] Q. Guo, C. Cheng, Z.-H. Sun, Z. Song, H. Li, Z. Wang, W. Ren, H. Dong, D. Zheng, Y.-R. Zhang, et al., *Nat. Phys.* **17**, 234 (2021).
[24] C. Zha, V. M. Bastidas, M. Gong, Y. Wu, H. Rong, R. Yang, Y. Ye, S. Li, Q. Zhu, S. Wang, et al., *Phys. Rev. Lett.* **125**, 1 (2020).
[25] K. Xu, J.-J. Chen, Y. Zeng, Y.-R. Zhang, C. Song, W. Liu, Q. Guo, P. Zhang, D. Xu, H. Deng, et al., *Phys. Rev. Lett.* **120** (2018).
[26] B. Chiaro, C. Neill, A. Bohrdt, M. Filippone, F. Arute, K. Arya, R. Babbush, D. Bacon, J. Bardin, R. Barends, et al., arXiv:1910.06024.
[27] Q. Guo, C. Cheng, H. Li, S. Xu, P. Zhang, Z. Wang, C. Song, W. Liu, W. Ren, H. Dong, et al., *Phys. Rev. Lett.* **127** (2021).
[28] M. Schreiber, S. S. Hodgman, P. Bordia, H. P. Lüschen, M. H. Fischer, R. Vosk, E. Altman, U. Schneider, and I. Bloch, *Science* **349**, 842 (2015).
[29] S. S. Kondov, W. R. McGehee, W. Xu, and B. DeMarco, *Phys. Rev. Lett.* **114**, 083002 (2015).
[30] P. Bordia, H. Lüschen, S. Scherg, S. Gopalakrishnan, M. Knap, U. Schneider, and I. Bloch, *Phys. Rev. X* **7**, 041047 (2017).
[31] P. Bordia, H. Lüschen, U. Schneider, M. Knap, and I. Bloch, *Nat. Phys.* **13**, 460 (2017).
[32] S. Choi, J. Choi, R. Landig, G. Kucsko, H. Zhou, J. Isoya, F. Jelezko, S. Onoda, H. Sumiya, V. Khemani, et al., *Nature* **543**, 221 (2017).
[33] J. Choi, H. Zhou, S. Choi, R. Landig, W. W. Ho, J. Isoya, F. Jelezko, S. Onoda, H. Sumiya, D. A. Abanin, et al., *Phys. Rev. Lett.* **122**, 043603 (2019).
[34] N. Defenu, T. Donner, T. Macrì, G. Pagano, S. Ruffo, and A. Trombettoni, arXiv:2109.01063.
[35] D. Lewis, A. Benhemou, N. Feinstein, L. Banchi, and S. Bose, *Phys. Rev. Lett.* **126**, 240502 (2021).
[36] F. Rajabi, S. Motlakunta, C.-Y. Shih, N. Kotibhaskar, Q. Quraishi, A. Ajoy, and R. Islam, *npj Quantum Inf.* **5**, 32 (2019).
[37] X. Deng, G. Masella, G. Pupillo, and L. Santos, *Phys. Rev. Lett.* **125**, 010401 (2020).
[38] S. Roy and D. E. Logan, *SciPost Phys.* **7** (2019).
[39] R. M. Nandkishore and S. L. Sondhi, *Phys. Rev. X* **7**, 041021 (2017).
[40] N. Y. Yao, C. R. Laumann, S. Gopalakrishnan, M. Knap, M. Müller, E. A. Demler, and M. D. Lukin, *Phys. Rev. Lett.* **113**, 243002 (2014).
[41] R. Modak and T. Nag, *Phys. Rev. E* **101**, 052108 (2020).
[42] A. L. Burin, *Phys. Rev. B* **92**, 104428 (2015).
[43] S. Schiffer, J. Wang, X.-J. Liu, and H. Hu, *Phys. Rev. A* **100**, 063619 (2019).
[44] A. L. Burin, *Phys. Rev. B* **91**, 094202 (2015).
[45] K. S. Tikhonov and A. D. Mirlin, *Phys. Rev. B* **97**, 214205 (2018).
[46] A. O. Maksymov and A. L. Burin, *Phys. Rev. B* **101**, 024201 (2020).
[47] H. Li, J. Wang, X.-J. Liu, and H. Hu, *Phys. Rev. A* **94**, 063625 (2016).
[48] H. Li, J. Wang, X.-J. Liu, and H. Hu, *Phys. Rev. A* **94**, 063625 (2016).
[49] J. H. Bardarson, F. Pollmann, and J. E. Moore, *Phys. Rev. Lett.* **109**, 017202 (2012).
[50] R. Modak and T. Nag, *Phys. Rev. Research* **2**, 012074 (2020).
[51] N. Roy and A. Sharma, *Phys. Rev. B* **97**, 125116 (2018).
[52] M. Serbyn, Z. Papić, and D. A. Abanin, *Phys. Rev. Lett.* **110**, 260601 (2013).
[53] M. Pino, *Phys. Rev. B* **90**, 174204 (2014).
[54] G. De Tomasi, *Phys. Rev. B* **99**, 054204 (2019).
[55] A. Safavi-Naini, M. L. Wall, O. L. Acevedo, A. M. Rey, and R. M. Nandkishore, *Phys. Rev. A* **99**, 033610 (2019).

- [56] R. Singh, R. Moessner, and D. Roy, Phys. Rev. B **95**, 094205 (2017).
- [57] S. Nag and A. Garg, Phys. Rev. B **99**, 224203 (2019).
- [58] L. D’Alessio and M. Rigol, Phys. Rev. X **4**, 041048 (2014).
- [59] A. Lazarides, A. Das, and R. Moessner, Phys. Rev. E **90**, 012110 (2014).
- [60] P. Ponte, A. Chandran, Z. Papić, and D. A. Abanin, Ann. Phys. **353**, 196 (2015).
- [61] A. Lazarides, A. Das, and R. Moessner, Phys. Rev. Lett. **115** (2015).
- [62] H. Burau, M. Heyl, and G. De Tomasi, Phys. Rev. B **104**, 224201 (2021).
- [63] L. Zhang, V. Khemani, and D. A. Huse, Phys. Rev. B **94**, 224202 (2016).
- [64] D. S. Bhakuni and A. Sharma, Phys. Rev. B **102**, 085133 (2020).
- [65] M. Sarkar, R. Ghosh, A. Sen, and K. Sengupta, arXiv:2107.11395.
- [66] M. Mierzejewski, K. Giergiel, and K. Sacha, Phys. Rev. B **96**, 140201 (2017).
- [67] P. Ponte, Z. Papić, F. m. c. Huvveneers, and D. A. Abanin, Phys. Rev. Lett. **114**, 140401 (2015).
- [68] E. Bairey, G. Refael, and N. H. Lindner, Phys. Rev. B **96** (2017).
- [69] S. Choi, D. A. Abanin, and M. D. Lukin, Phys. Rev. B **97**, 100301 (2018).
- [70] D. S. Bhakuni, R. Nehra, and A. Sharma, Phys. Rev. B **102** (2020).
- [71] P. Jurcevic, B. P. Lanyon, P. Hauke, C. Hempel, P. Zoller, R. Blatt, and C. F. Roos, Nature **511**, 202 (2014).
- [72] P. Richerme, Z.-X. Gong, A. Lee, C. Senko, J. Smith, M. Foss-Feig, S. Michalakis, A. V. Gorshkov, and C. Monroe, Nature **511**, 198 (2014).
- [73] V. Oganesyan and D. A. Huse, Phys. Rev. B **75**, 155111 (2007).
- [74] L. D’Alessio and M. Rigol, Phys. Rev. X **4**, 041048 (2014).
- [75] A. Sorge, pyfssa 0.7.6. Zenodo. (2015).
- [76] O. Melchert, arXiv:0910.5403.
- [77] N. Laflorencie, arXiv:2112.09102.

Supplementary Materials: Non-algebraic entanglement growth in long-range many-body localized systems

In the main text, we discussed how the critical τ_c 's are precisely determined through finite-size scaling analysis for considered systems. In Figs. S1(a)-(b) we plot $\langle r \rangle$ as a function of τ for two choices of uniform (namely $a = b$) couplings $a = 1$ and $a = 1.25$, respectively. Clearly, the curves for different sizes do not show clear intersection at a specific τ and the finite-size scaling analysis (insets of Figs. S1(a)-(b)) fails to collapse the curves exactly, for all choices of other parameters, indicating the absence of MBL transition. This shows that for $a < 1.5$ the thermalizing long-range tunneling overcomes the localizing long-range Ising and, hence, the MBL can not be observed.

As we discussed in the main text, in systems with nonuniform couplings ($b \ll a \rightarrow \infty$) by decreasing b (i.e. making the Ising interaction more long-range) the localization power increases and the system can localize for longer τ . Figs. S1(c)-(d) presents $\langle r \rangle$ vs τ for two choices of $b = 0.5$ and $b = 1$, respectively. For considered system sizes, one can see the clear intersection points for all the curves which determine the onset of transition. The finite-size scaling analysis which collapses all the curves on a universal one as a function of $(\tau - \tau_c)L^{1/\nu}$ and leads to precise τ_c is presented in the insets of Figs. S1(c)-(d).

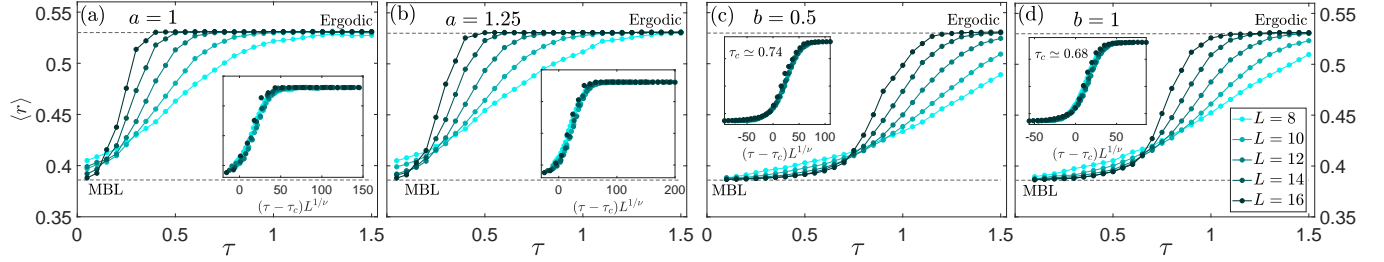


FIG. S1: Random-averaged level statistics ratio $\langle r \rangle$ as a function of τ for different system sizes $L = 8, \dots, 16$ when the strength of the disordered kick is fix to $\theta = \pi$. In panels (a) and (b), the couplings of the system are uniform with values $a = b = 1$ and 1.25 . In panels (c) and (d), the couplings are nonuniform with $a \rightarrow \infty$ and $b = 0.5$ and 1 .